

Review

The effect of ceramic in combinations of two sigmoid functionally graded rotating disks with variable thickness

Aidy Ali^{1*}, M. Bayat¹, B. B. Sahari¹, M. Saleem² and O. S. Zaroog³

¹Department of Mechanical Engineering, Universiti Pertahanan Nasional Malaysia, Kem Sungai Besi, 57000 UPM, Kuala Lumpur, Malaysia.

²Department of Applied Mathematics, Z.H. College of Engineering and Technology, A.M.U., India.

³Department of Mechanical Engineering, Universiti Tenaga Nasional, 43009 Kajang, Selangor, Malaysia.

Accepted 30 May, 2012

This paper present the elastic solutions of the disk made of functionally graded material (FGM) with variable thickness subjected to rotating load. The material properties are presented by combination of two sigmoid FGM (S-FGM) and disk thickness profile are assumed to be represented by power law distributions. Aluminum-ceramic-aluminum FG rotated disk is considered. Hollow disks are considered and the solutions for the stresses and displacements are given under appropriate boundary conditions. The results in metal-ceramic-metal FGMs are presented and compared with the known results in the literature. The solutions for S-FGM are compared with that of non FGM, and for variable thickness and for uniform thickness. The effects of the material grading index, n , and the geometry of the disk on the stress and displacement are investigated. It is found that a FG disk with concave thickness profile has smaller stresses and displacements compared with the concave or linear by variable thickness profile. The results in metal-ceramic or ceramic-metal and metal-ceramic-metal FGMs are compared. These results suggest that a rotating FG disk with metal-ceramic-metal can be more efficient than the one with ceramic-metal or metal-ceramic.

Key words: Rotating disk, variable thickness, elasticity, sigmoid functionally graded material.

INTRODUCTION

Functionally graded materials (FGMs) are defined as those materials in which the volume fraction of the two or more materials is varied, as a power-law, sigmoid or exponential distribution, continuously as a function of position along certain dimension(s) of the structure (Reddy, 2000; Suresh and Mortensen, 1998). These materials are mainly constructed to operate in high temperature environments.

Rotating disks have many practical engineering applications such as in steam and gas turbine rotors, turbo generators, internal combustion engines, fly wheels, turbojet engines, reciprocating and centrifugal compressors

just to mention a few. Brake disk can be an example of solid rotating disk where only body force is involved. Solid disks can also be found in components such as cover plates of rotating components and idlers used in belt assemblies.

In a turbine rotor, there is always a possibility that the heat from the external surface transmits to the shaft and from it to the bearings causing adverse effects on its function and efficiency. To deal with this situation and to prevent heat from being transferred to the shaft and bearings, the disk can be made of FGM with ceramic-rich at the outer surface and metal-rich at the inner surface. While the heat resistant property of the ceramic at the outer surface prevents heat from being transferred, the metal at the inner surface helps carry the stress for the transmission of torque from the disk to the shaft.

The boundary conditions of the disk depend on the way

*Corresponding author. E-mail: aidyali@upnm.edu.my. Tel: +60172496293. Fax: +60 3 86567122.

the disk is attached to the shaft. For a disk connected rigidly to the shaft (by means of welding or shaft and rotor disk cast together), a fixed-free condition applies. On the other hand, for the disk connected to the shaft by means of splines where small axial movement is allowed, a free-free condition applies. Flywheels and gear wheels are other examples of fixed-free conditions usually used for storing kinetic energy and transmitting mechanical power, respectively.

In any of the mentioned applications, the performance of the component in terms of efficiency, service life and power transmission depends on the material, speed of rotation and operating conditions. Normally, a component can be fabricated using any metal. However, for some specific applications such as in aerospace engineering where the component's weight and durability in high temperature environment are so crucial, the components need to be fabricated using special material such as a FGM. FGMs are usually made of a mixture of ceramic and metals. The ceramic constituent of the material provides the high temperature resistance due to its low thermal conductivity. The ductile metal constituent, on the other hand, prevents fracture caused by stress due to high temperature gradient in a very short period of time (Reddy et al., 1999).

Fukui et al. (1993) considered a thick-walled FG tube under uniform thermal loading and investigated the effect of graded components on residual stresses. They further estimated the optimum composition gradient generated by compressive circumferential stress at the inner surface. Boussaa (2000) investigated the problem of optimizing the composition profile of a FG interlayer inserted between a metallic tube and a ceramic coating so as to alleviate the thermal stresses occurring at the metal-ceramic interface. Jabbari et al. (2003) presented the general theoretical analysis of two-dimensional steady-state thermal stresses for a hollow thick cylinder made of FGM.

Horgan and Chan (1999) investigated the effects of material inhomogeneity on the response of linearly-elastic isotropic solid circular disks or cylinders rotating at constant angular velocity about its axis of symmetry. A special case of a body with Young's modulus depending on the radial coordinate only and constant Poisson's ratio was examined. For the case when the Young's modulus had a power-law dependence on the radial coordinate, explicit exact solutions were obtained.

Many studies conducted on FGMs were related to the analysis of thermal stresses and deformations (Liew et al., 2003; Ootao and Tanigawa, 1999; Ootao and Tanigawa, 2004; Shahsiah and Eslami, 2003). Ruhi et al. (2005) presented a semi-analytical thermo elastic solution for finitely long thick-walled cylinders made of FGMs.

Durodola and Attia (2000a, b) presented a finite element analysis for FG rotating disks using commercial software package. The disks were modeled as non-

homogeneous orthotropic materials such as those obtained through non-uniform reinforcement of metal matrix by long fibers. They considered three types of gradation distributions of the Young's modulus E in the hoop direction relative to matrix material modulus. Kordkheili and Naghdabadi (2007) presented semi-analytical thermo elastic solutions for hollow and solid rotating axisymmetric disks made of FGMs under plane stress condition. They compared their results with those of Durodola and Attia (2000a, b) under the centrifugal loading.

Although many earlier studies on rotating disks (Tutuncu, 1995) have considered disks with uniform thickness, several authors have emphasized the importance of variable thickness in the rotating disks (Eraslan, 2003; Eraslan and Argeso, 2002; Guven, 1992; Reddy and Srinath, 1974). Recent studies (Eraslan and Orcan, 2002; Orcan and Eraslan, 2002) indicated that stresses in rotating disks (annular or solid) with variable thickness are much lower than those in a uniform-thickness disk at the same angular velocity. Jahed et al. (2005) analyzed an inhomogeneous disk model with variable thickness to achieve minimum weight of disk. Using the variable material properties method, stresses were obtained for the disk under rotation and a steady temperature field. Bayat et al. (2008) analyzed the FG gear wheel with variable thickness using material properties as a single power-law FGM (P-FGM).

To the best of authors' knowledge, no work has been reported to date which concerns with the analysis of the combination of two sigmoid FG (S-FG) disks with variable thickness. This very fact motivates the present study. In this paper, a thin FG disk with variable thickness (Figure 1) subjected to centrifugal loading due to constant angular velocity is considered. The thickness of the disk is assumed to be sufficiently small compared to its diameter and plane stress condition is applied. The symmetry with respect to the rotational axis and the mid-plane is assumed. This work aims to investigate the effect of combination of two S-FGMs and property gradation and also the geometry of the disk on stresses and displacements in hollow disks under free-free and fixed-free boundary conditions. The non-dimensional stress and displacement components in the radial direction are given using semi-analytical method based on the form of the sigmoid distribution for the mechanical properties of the constituent components and hyperbolic distribution for the thickness profile.

To implement the semi-analytical method in numerical studies, the radial domain of the disk is divided into some virtual sub-domains where, in each sub-domain, the mechanical property is assumed to be constant. This assumption yields the governing equilibrium equations in each sub-domain as ordinary differential equations with constant coefficients whose general solution can be written involving certain unknowns. These unknowns can be determined as solution of systems of linear algebraic

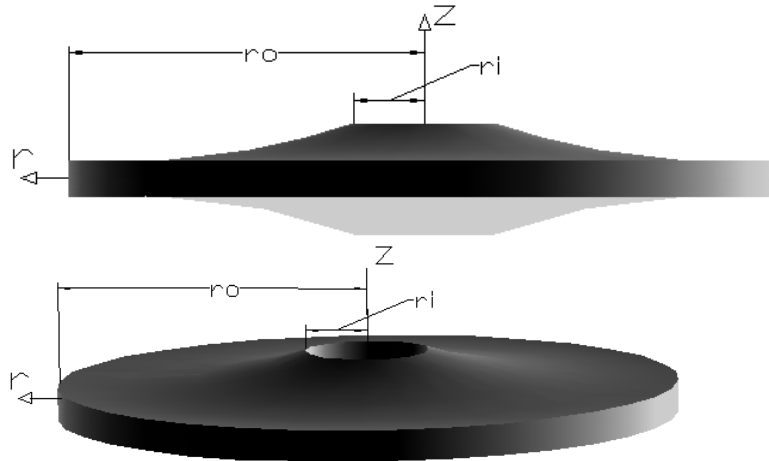


Figure 1. Configuration of a thin disk with variable thickness.

equations obtained by imposing the continuity conditions at the interface of the adjacent sub-domains together with global conditions. Increasing the number of sub-domains (divisions) in the radial direction increases the accuracy in the solution.

GRADATION RELATION

In this study, the property variation P of the material in the FG disk along the radial direction is assumed to be the following form (Chi and Chung, 2006):

$$P(r) = g_1(r)P_1 + (1 - g_1(r))P_2 ; r_1 < r < \bar{r} \tag{1a}$$

$$P(r) = g_2(r)P_1 + (1 - g_2(r))P_2 ; \bar{r} < r < r_2 \tag{1b}$$

Where

$$g_1(r) = 1 - \frac{1}{2} \left(\frac{r - r_1}{\bar{r} - r_1} \right)^n ; r_1 < r < \bar{r} \tag{1c}$$

$$g_2(r) = \frac{1}{2} \left(\frac{r_2 - r}{r_2 - \bar{r}} \right)^n ; \bar{r} < r < r_2 \tag{1d}$$

$$\bar{r} = \frac{r_2 + r_1}{2} \tag{1e}$$

Here, P_1 and P_2 are the corresponding properties of materials 1 and 2 of the disk; r_1 and r_2 are the radius that

there exist full materials 1 and 2, respectively; $n \geq 0$ is the volume fraction exponent (also called grading index in this paper); $g(r)$ is power law function; \bar{r} is the mean radius of r_1 and r_2 . In this study, the Poisson's ratio ν is assumed to be constant and the elastic modulus E and the density ρ are assumed to vary according to the gradation relations (1), for example, the assumed form for the modulus of elasticity E is:

$$E(r) = g_1(r)E_1 + (1 - g_1(r))E_2 ; r_1 < r < \bar{r} \tag{2a}$$

$$E(r) = g_2(r)E_1 + (1 - g_2(r))E_2 ; \bar{r} < r < r_2 \tag{2b}$$

By using Equations 1 and considering two types of S-FGMs, first aluminum-ceramic between r_i (inner radius of the disk) and $\frac{r_o + r_i}{2}$ (r_o is outer radius of disk); second ceramic-aluminum between $\frac{r_o + r_i}{2}$ and r_o . The variation of non-dimensional modulus of elasticity, $\frac{E}{E_c}$, with non-dimensional radial distance, $\frac{r}{r_o}$, is shown in Figure 2.

The thickness-profile h of the disk is assumed to vary radially according to the following form:

$$h(r) = h_o \left(1 - \left(\frac{r}{q + r_o} \right)^m \right) \tag{3a}$$

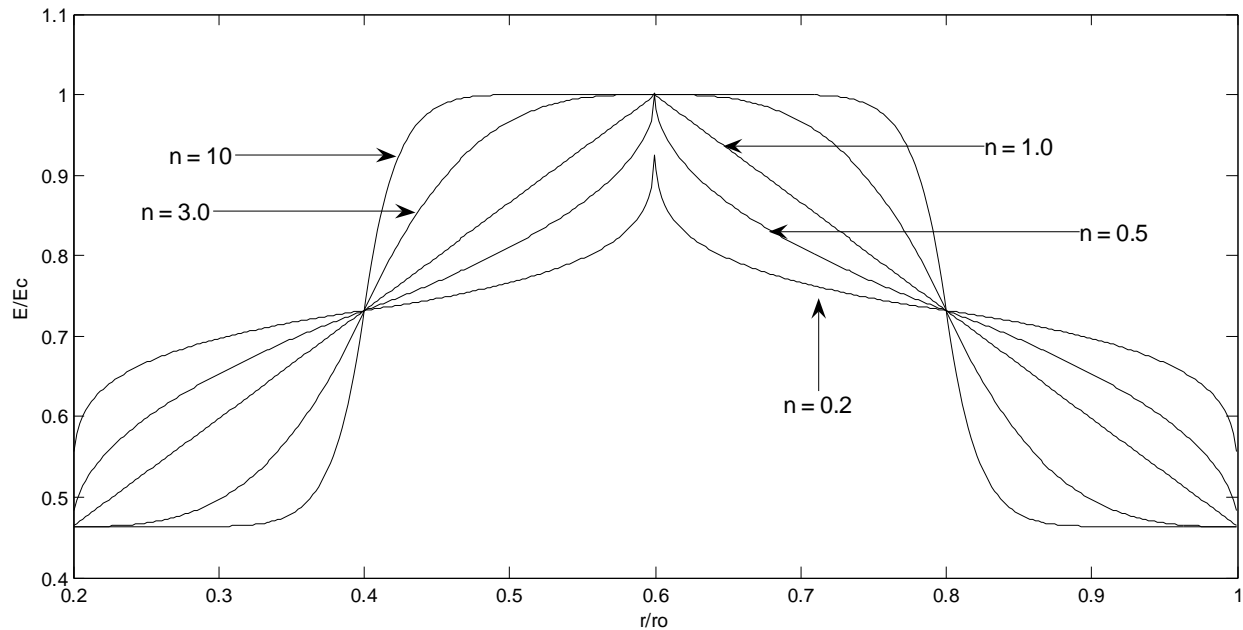


Figure 2. Variation of the non-dimensional elastic modulus versus non-dimensional radius.

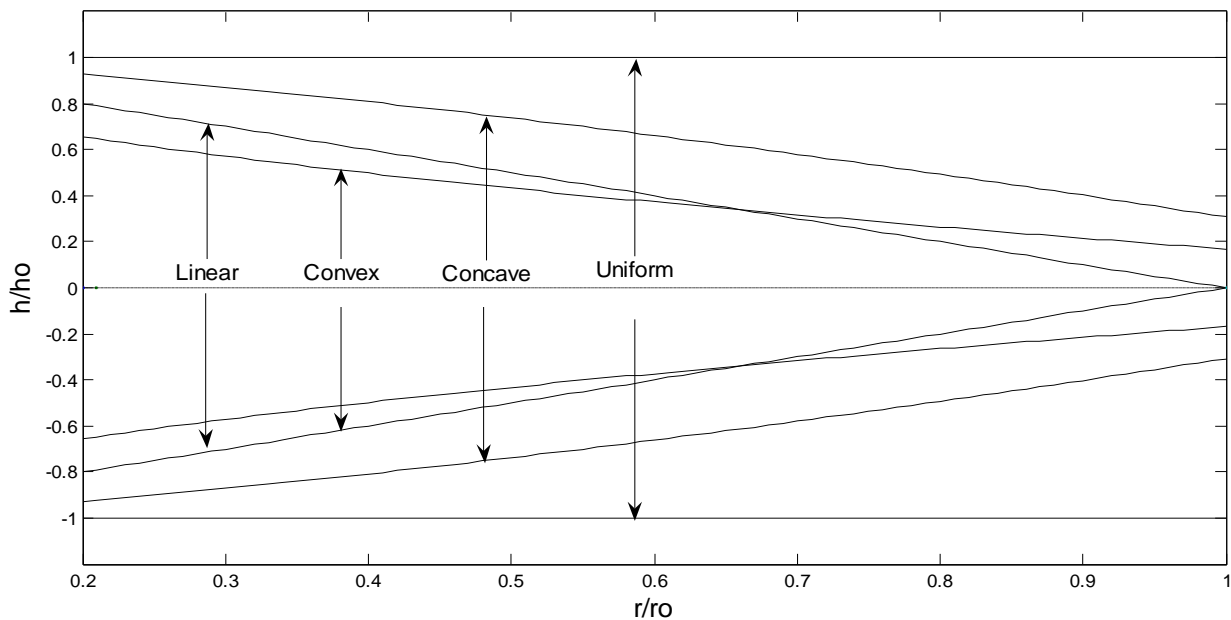


Figure 3. Variation of non-dimensional thickness versus non-dimensional radius.

Here, q and m are geometric parameters such that $0 \leq q < 1, m > 0$; h_0 is the thickness at the axis of the disk. A uniform thickness disk can be obtained by setting $q \neq 0, m \rightarrow \infty$. A linearly decreasing thickness can be obtained for $m = 1$. The profile is

concave if $m < 1$ and it is convex if $m > 1$. Different forms of the thickness profiles are shown in Figure 3.

For a future reference, another important parameter that is, the ratio of the weight of the double S-FG disk, W , and the weight of all-ceramic disk of same size, W_{Cer} , denoted by W/W_{Cer} can be defined as:

$$\begin{aligned}
 W/W_{Cer} = & \int_{r_i}^{\frac{3r_i+r_o}{4}} r(g_1(r)\rho_{Al} + (1-g_1(r))\rho_{Cer}) \left(1 - \left(\frac{r}{q+r_o}\right)^m\right) dr + \int_{r_i}^{r_o} r \left(\rho_{Cer} \left(1 - \left(\frac{r}{q+r_o}\right)^m\right)\right) dr + \\
 & + \int_{\frac{3r_i+r_o}{4}}^{\frac{r_i+r_o}{2}} r(g_2(r)\rho_{Al} + (1-g_2(r))\rho_{Cer}) \left(1 - \left(\frac{r}{q+r_o}\right)^m\right) dr + \int_{r_i}^{r_o} r \left(\rho_{Cer} \left(1 - \left(\frac{r}{q+r_o}\right)^m\right)\right) dr + \\
 & + \int_{\frac{r_i+3r_o}{2}}^{\frac{r_i+r_o}{4}} r(g_1(r)\rho_{Cer} + (1-g_1(r))\rho_{Al}) \left(1 - \left(\frac{r}{q+r_o}\right)^m\right) dr + \int_{r_i}^{r_o} r \left(\rho_{Cer} \left(1 - \left(\frac{r}{q+r_o}\right)^m\right)\right) dr + \\
 & + \int_{\frac{r_i+3r_o}{4}}^{r_o} r(g_2(r)\rho_{Cer} + (1-g_2(r))\rho_{Al}) \left(1 - \left(\frac{r}{q+r_o}\right)^m\right) dr + \int_{r_i}^{r_o} r \left(\rho_{Cer} \left(1 - \left(\frac{r}{q+r_o}\right)^m\right)\right) dr \quad (3b)
 \end{aligned}$$

with ρ_{Cer} denoting the density of the all-ceramic disk. W/W_{Cer} will be used to compare the weights of FG disks with the weight of all-ceramic disk in the following sections.

THEORETICAL FORMULATION AND EQUILIBRIUM EQUATIONS

Consider a hollow axial symmetric FG disk with variable thickness with inner radius r_i and outer radius r_o , as shown in Figure 1. The disk rotates at an angular velocity ω . The problem is assumed to be plane stress. Due to the axial symmetry assumptions in geometry and loading, cylindrical coordinate system (r, θ, z) is used. The inner and outer surfaces of the FG disk are assumed to be metal-rich and at radius \bar{r} ceramic-rich is assumed. Between these two surfaces, the material properties vary according to Equations 1.

It may be mentioned that although a metal-rich at the inner and outer surfaces and full-ceramic at mid way between inner and outer surfaces, material gradient has been considered for all the disks in this paper. The method of solution that has been followed is independent of such a gradient and may be applied to other gradients as well. However, several applications considered in this paper such as an FG gear wheel mounted on a shaft-support justify consideration of metal-rich inner and outer surface of the disks. Also, for an FG gear wheel mounted on shaft-support ductility plays an important role and thus the metal dominated inner and outer surface of the disk is further justified.

Strains and displacement field

Using the infinitesimal theory of elasticity and the rotational symmetry, the strain-displacement relations are:

$$\epsilon_r = \frac{du}{dr} \quad (4a)$$

$$\epsilon_\theta = \frac{u}{r} \quad (4b)$$

Where u is the radial displacement. Also, the linear constitutive elastic equations in the cylindrical coordinate are used in the form of:

$$\sigma_r = \frac{E(r)}{1-\nu^2} (\epsilon_r + \nu\epsilon_\theta) \quad (5a)$$

$$\sigma_\theta = \frac{E(r)}{1-\nu^2} (\epsilon_\theta + \nu\epsilon_r) \quad (5b)$$

Where E is the modulus of elasticity and ν is the Poisson’s ratio.

Equilibrium equations

For a rotating disk, if U_1 is the total strain energy of the body and V_1 is the total potential energy of external force, then the total energy Π can be represented as:

$$\Pi = U_1 + V_1 \quad (6)$$

The principle of minimum total potential energy states:

$$\delta(U_1 + V_1) \equiv \delta\Pi = 0 \quad (7)$$

And this yield

$$\delta U_1 = \int_V \sigma_{ij} \delta \epsilon_{ij} dV = \int_{r_i}^{r_o} \int_{-h(r)/2}^{h(r)/2} 2\pi(\sigma_r \delta \epsilon_r + \sigma_\theta \delta \epsilon_\theta) r dz dr = \int_{r_i}^{r_o} \int_{-h(r)/2}^{h(r)/2} 2\pi(\sigma_r \delta(\frac{du}{dr}) + \sigma_\theta \delta(\frac{u}{r})) r dz dr \quad (8)$$

Here, V represents the total volume of disk. For the body force, the potential energy of applied load is given by:

$$\delta V_1 = -(2\pi \int_{r_i}^{r_o} \int_{-h/2}^{h/2} \rho r \omega^2 r dz dr) \delta u \quad (9)$$

Substituting for U_1 and V_1 form Equations 8 and 9 into Equation 7, and integrating once, one gets

$$\frac{d}{dr} (h(r)r\sigma_r) - h(r)\sigma_\theta + h(r)\rho(r)\omega^2 r^2 = 0 \quad (10)$$

The equilibrium equation is obtained, the results is the same as Reddy and Srinath (1974) and yields the Navier equation for the radial displacement as follows:

$$rh_r E_r \frac{d^2 u}{dr^2} + \left(r E_r \frac{dh_r}{dr} + r h_r \frac{dE_r}{dr} + E_r h_r \right) \frac{du}{dr} + \left(\nu E_r \frac{dh_r}{dr} + \nu h_r \frac{dE_r}{dr} - \frac{1}{r} E_r h_r \right) u + (1 - \nu^2) h_r \rho_r r^2 \omega^2 = 0 \quad (11)$$

Here, for brevity, symbols h_r , E_r and ρ_r have been used for the functions $h(r)$, $E(r)$ and $\rho(r)$ respectively. In Equation 11, the displacement u is a function of r only due to axial symmetry and plane stress condition.

BOUNDARY CONDITIONS

Hollow disk free-free

The following traction conditions on the inner and outer surfaces of the rotating hollow disk must be satisfied.

$$\begin{aligned} \sigma_r = 0 \quad r = r_i \\ \sigma_r = 0 \quad r = r_o \end{aligned} \quad (12)$$

Hollow disk fixed-free

$$\begin{aligned} u = 0 \quad r = r_i \\ \sigma_r = 0 \quad r = r_o \end{aligned} \quad (13)$$

NON-DIMENSIONAL FORM

Navier Equation 11 and the boundary conditions given by Equations 12 and 13 can be written in non-dimensional form using the following set of variables:

$$R = \frac{r}{r_o}, H_R = \frac{h_r}{h_o}, \overline{E}_R = \frac{E_r}{E_c}, U = \frac{u}{u_o}, \overline{\rho}_R = \frac{\rho_r}{\rho_c} \quad (14)$$

Where

$$u_o = \frac{\rho_c r_o^3 \omega^2}{E_c}$$

The non-dimensional form of Equation 4 is then given by:

$$\begin{aligned} RH_R \overline{E}_R \frac{d^2 U}{dR^2} + \left(R \overline{E}_R \frac{dH_R}{dR} + RH_R \frac{d\overline{E}_R}{dR} + \overline{E}_R H_R \right) \frac{dU}{dR} + \left(\nu \overline{E}_R \frac{dH_R}{dR} + \nu H_R \frac{d\overline{E}_R}{dR} - \frac{1}{R} \overline{E}_R H_R \right) U + (1 - \nu^2) H_R \overline{\rho}_R R^2 = 0 \end{aligned} \quad (15)$$

Where

$$\overline{E}_R = g_1(r) \overline{E}_{R_i} - g_1(r) + 1; \quad r_i < r < \frac{3r_i + r_o}{4}$$

$$\overline{E}_R = g_2(r) \overline{E}_{R_i} - g_2(r) + 1; \quad \frac{3r_i + r_o}{4} < r < \frac{r_i + r_o}{2}$$

$$\overline{E}_R = g_1(r) + (1 - g_1(r)) \overline{E}_{R_i}; \quad \frac{r_i + r_o}{2} < r < \frac{r_i + 3r_o}{4}$$

$$\overline{E}_R = g_2(r) + (1 - g_2(r)) \overline{E}_{R_i}; \quad \frac{r_i + 3r_o}{4} < r < r_o$$

$$\overline{E}_{R_i} = \frac{E_{al}}{E_c}$$

$$H_R = R^{-m} \quad (16)$$

Non-dimensional boundary conditions

Hollow disk free-free

For this case, the boundary conditions of Equation 12 reduce to

$$\begin{aligned} \overline{\sigma}_R = \frac{\overline{E}_R}{1 - \nu^2} \left(\frac{dU}{dR} + \nu \frac{U}{R} \right) = 0 \quad R = R_i \quad \overline{\sigma}_R = 0 \\ R = 1 \end{aligned} \quad (17)$$

Hollow disk fixed-free

Boundary conditions of Equation 13 turn out to be

$$\begin{aligned} U = 0 \quad R = R_i \\ \overline{\sigma}_R = 0 \quad R = 1 \end{aligned} \quad (18)$$

It may be noted that the study of Equation 15 in non-dimensional form makes the absolute values of properties and the loading speed unimportant.

ELASTIC SOLUTION

A closed-form solution of Equation 15 with variable coefficients seems to be difficult, if not impossible, to obtain. The method of analysis is the same as describe in Bayat et al. (2008). However, for completeness of the present paper, the method is also presented here.

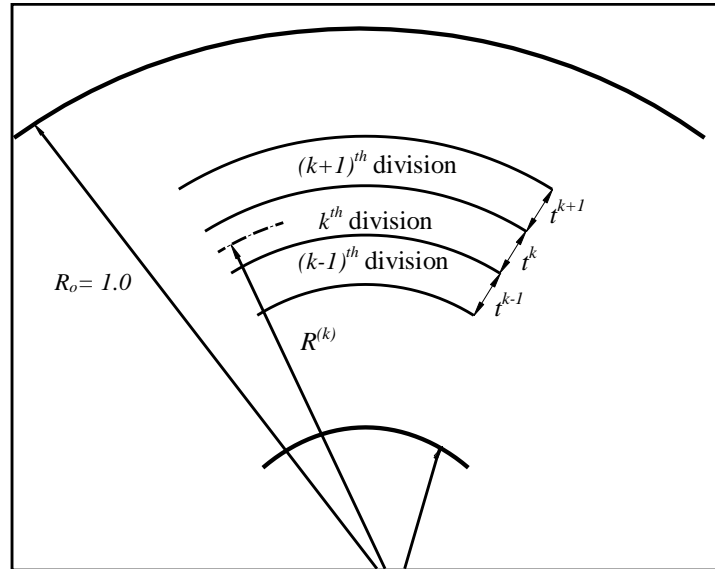


Figure 4. Dividing radial domain into some finite sub-domains.

Hence, in this study a semi-analytical solution of Equation 15 is attempted. In this method, a disk is divided into some virtual sub-domains (say q), with $t^{(k)}$ denoting the radial-width of the k^{th} sub-domain as shown in Figure 4. Evaluating the coefficients of Equation 15 at $R = R^{(k)}$, the mean radius of the k^{th} division, an ordinary differential equation with constant coefficients is obtained which is valid in k^{th} sub-domain. That is:

$$\left(c_1^{(k)} \frac{d^2}{dR^2} + c_2^{(k)} \frac{d}{dR} + c_3^{(k)} \right) U^{(k)} + c_4^{(k)} = 0, \quad (19)$$

Where

$$\begin{aligned} c_1^{(k)} &= R^{(k)} H_{R^{(k)}} \overline{E_{R^{(k)}}} \\ c_2^{(k)} &= R^{(k)} \overline{E_{R^{(k)}}} \frac{dH_R}{dR} \Big|_{R=R^{(k)}} + R^{(k)} H_{R^{(k)}} \frac{d\overline{E_R}}{dR} \Big|_{R=R^{(k)}} + H_{R^{(k)}} \overline{E_{R^{(k)}}} \\ c_3^{(k)} &= \nu \overline{E_{R^{(k)}}} \frac{dH_R}{dR} \Big|_{R=R^{(k)}} + \nu H_{R^{(k)}} \frac{d\overline{E_R}}{dR} \Big|_{R=R^{(k)}} - \frac{1}{R^{(k)}} H_{R^{(k)}} \overline{E_{R^{(k)}}} \\ c_4^{(k)} &= (1-\nu^2) H_{R^{(k)}} \overline{\rho_{R^{(k)}}} (R^{(k)})^2. \end{aligned} \quad (20)$$

Using the mentioned technique, Equation 15 with variable Coefficients is changed into a system of q ordinary

differential equations with constant coefficients with q being the number of virtual sub-domains.

The solution for Equation 19 can be written in the form of:

$$U^{(k)} = X_1^{(k)} \exp(\lambda_1^{(k)} R) + X_2^{(k)} \exp(\lambda_2^{(k)} R) - \frac{c_4^{(k)}}{c_3^{(k)}}, \quad (21)$$

Where $X_1^{(k)}$ and $X_2^{(k)}$ are unknown constants for k^{th} sub-domain and

$$\lambda_1^{(k)}, \lambda_2^{(k)} = -\frac{c_2^{(k)} \pm \sqrt{(c_2^{(k)})^2 - 4c_3^{(k)} c_1^{(k)}}}{2c_1^{(k)}}$$

Also, the solution of Equation 21 is valid for

$$R^{(k)} - \frac{t^{(k)}}{2} \leq R \leq R^{(k)} + \frac{t^{(k)}}{2}. \quad (22)$$

Where $R^{(k)}$ and $t^{(k)}$ are the mean radius and the radial-width of the k^{th} sub-domain, respectively. The unknowns $X_1^{(k)}$ and $X_2^{(k)}$ can be determined by applying the necessary conditions between each two adjacent sub-domains. For this purpose, the continuity of the radial displacement U as well as radial stress $\overline{\sigma_R}$ is imposed at the interfaces of the adjacent sub-domains. The continuity conditions at interfaces are given by:

Table 1. Different cases of thickness profiles.

Variable	$m < 1$	$q \neq 0, m \rightarrow \infty$	$m > 1$	$m = 1$
	Case(a)	Case (b)	Case (c)	Case (d)
Thickness profile (Equation 3a)	Parabolic concave	Constant thickness	Parabolic convex	Linear

Table 2. Variation of non-dimensional weight with grading index n and thickness profile.

Thickness profile (Equation 2) Cases	Values of weight ratio, W/W_c , (Equation 3b)				
	Full-metal	$n = 1$	$n = 5.0$	Full-metal, full-ceramic, full-metal	Full-ceramic
a) Parabolic concave	0.4737	1194/1580 = 0.7559	1207/1580 = 0.7641	1209/1580 = 0.7652	1
b) Uniform	0.4737	2016/2736 = 0.7368	2016/2736 = 0.7368	2016/2736 = 0.7368	1
c) Parabolic convex	0.4737	684/909 = 0.7525	690/909 = 0.7591	692/909 = 0.7613	1
d) Linear	0.4737	659/851 = 0.7444	673/851 = 0.7908	675/851 = 0.7932	1

$$\begin{aligned}
 U^{(k)} \Big|_{R=R^{(k)+\frac{r^{(k)}}{2}}} &= U^{(k)} \Big|_{R=R^{(k+1)-\frac{r^{(k+1)}}{2}}} \\
 \overline{\sigma}_R^{(k)} \Big|_{R=R^{(k)+\frac{r^{(k)}}{2}}} &= \overline{\sigma}_R^{(k)} \Big|_{R=R^{(k+1)-\frac{r^{(k+1)}}{2}}}
 \end{aligned}
 \tag{23}$$

These conditions together with the global boundary conditions of Equation 17 or Equation 18 yield a set of linear algebraic equations in $X_1^{(k)}$ and $X_2^{(k)}$. Solving these equations for $X_1^{(k)}$ and $X_2^{(k)}$ and substituting them in Equation 21, the displacement component, U , is determined in each sub-domain. Increasing the number of divisions improves the accuracy of the results.

NUMERICAL RESULTS

For numerical illustration of the elastic solutions of this study, it is assumed that all the disks considered have the same volume. The same volume of the disks can be achieved by suitably choosing the value of h_o . It can be noted that the results obtained in this study are based on the non-dimensional formulation and thus are independent from the absolute value of h_o .

Two cases namely hollow disk free-free, hollow disk fixed-free are considered. The analysis is conducted using aluminum as the inner-surface metal and Zirconia as outer-surface ceramic the same as that considered by Bayat et al. (2008). The material properties are:

$$\begin{aligned}
 E_{Al} &= 70.0 \text{ GPa} & , & & E_{Cer} &= 151.0 \text{ GPa} \\
 \rho_{Al} &= 2700.0 \text{ kg/m}^3 & , & & \rho_{Cer} &= 5700.0 \text{ kg/m}^3 & , & \nu &= 0.3
 \end{aligned}
 \tag{24}$$

A hollow disk with $R_o = 5R_i$ or a solid disk rotating at

constant angular velocity is considered here. Different cases for the thickness profiles used in numerical illustrations are shown in Table 1.

The following four sets of parameter values for m (each set representing a particular case of Table 1) are considered.

$$a : q = 0.30, m = 1.4$$

$$b : q \neq 0.0, m \rightarrow \infty$$

$$c : q = 0.4, m = 0.55$$

$$d : m = 1.0 \tag{25}$$

The elastic deformation of disk with variable thickness due to rotation is determined. The effect of grading index, n , and variable thickness on the non-dimensional weight of the hallow disk is shown in Table 2. It can be seen that all-ceramic disks are the heaviest whereas full-metal disk is the lightest. The weight of FG disk is in between the all-ceramic and all-metal values.

For the values chosen for q and m as given in Equation 25, each thickness profile of the disk has 70% thickness reduction at the outer surface. The effect of thickness profile on the weight can be shown by comparing the weight values for the same value of grading index n . It can be noted both numerators and denominators are changed, by considering the numerators: it is seen that hollow FG disk with linear thickness profile has smaller weight compared to that with other thickness profiles; Figure 3 may be referred to for more details. To show the effect of grading index n on the weight, disks with the same thickness profile are considered. It is noticed that the weights of FG disks lie in

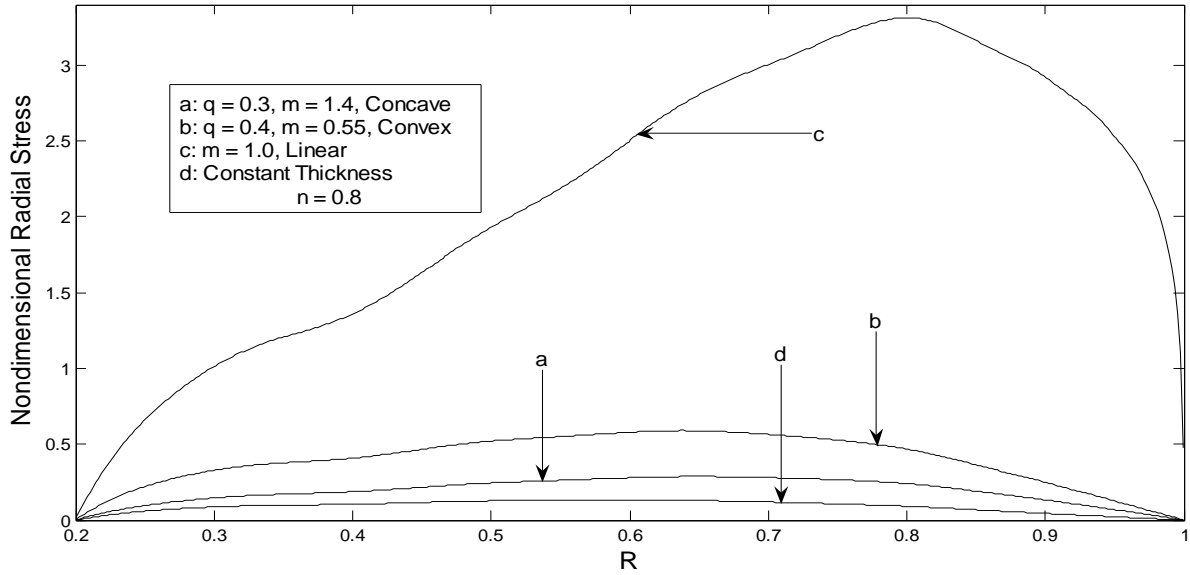


Figure 5. Variation of $\bar{\sigma}_R$ versus R for free-free hollow disk in the FG disk with variable thickness for different values of the geometric parameters q and m .

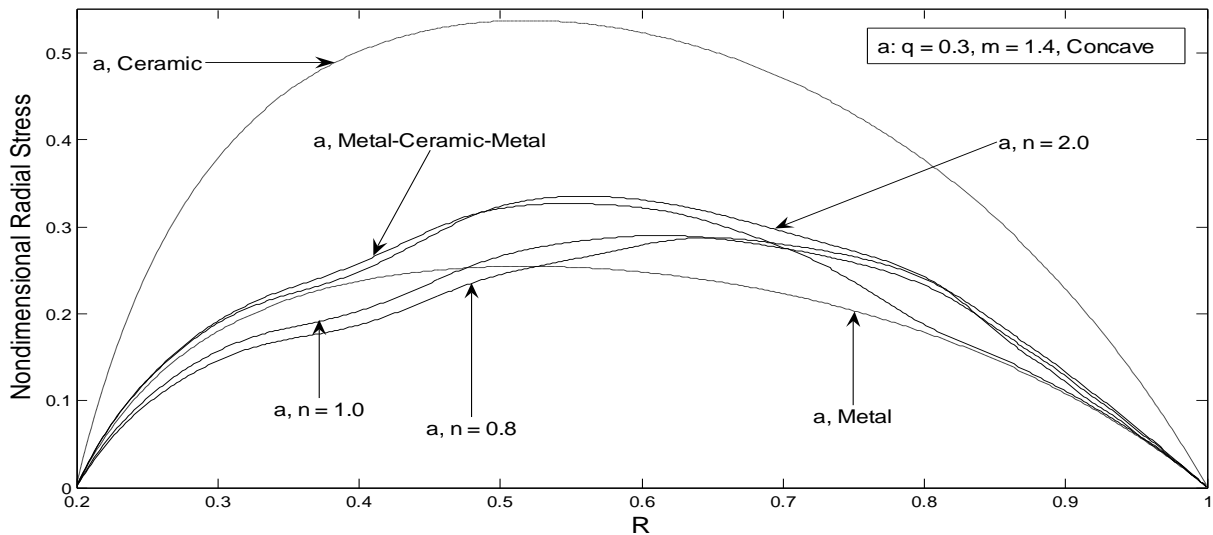


Figure 6. Variation of $\bar{\sigma}_R$ versus R for free-free hollow disk in the disk with concave thickness profile for different values of the grading index n .

between 0.4737 and 1, where $\frac{\rho_m}{\rho_c} = \frac{2700}{5700} = 0.4737$. In

this study, the density of ceramic is greater than the density of aluminum. It can be noted that for materials

such that $\frac{\rho_m}{\rho_c} > 1$, the weight of FG disk can be made even lighter than the full-metal disk.

It may be mentioned here that the method of solution considered in this study is general in nature and is not limited to gradients considered in this study only but can be applied to other gradients as well.

Hollow disk (Free-free)

Figures 5 and 6 show the non-dimensional radial stress

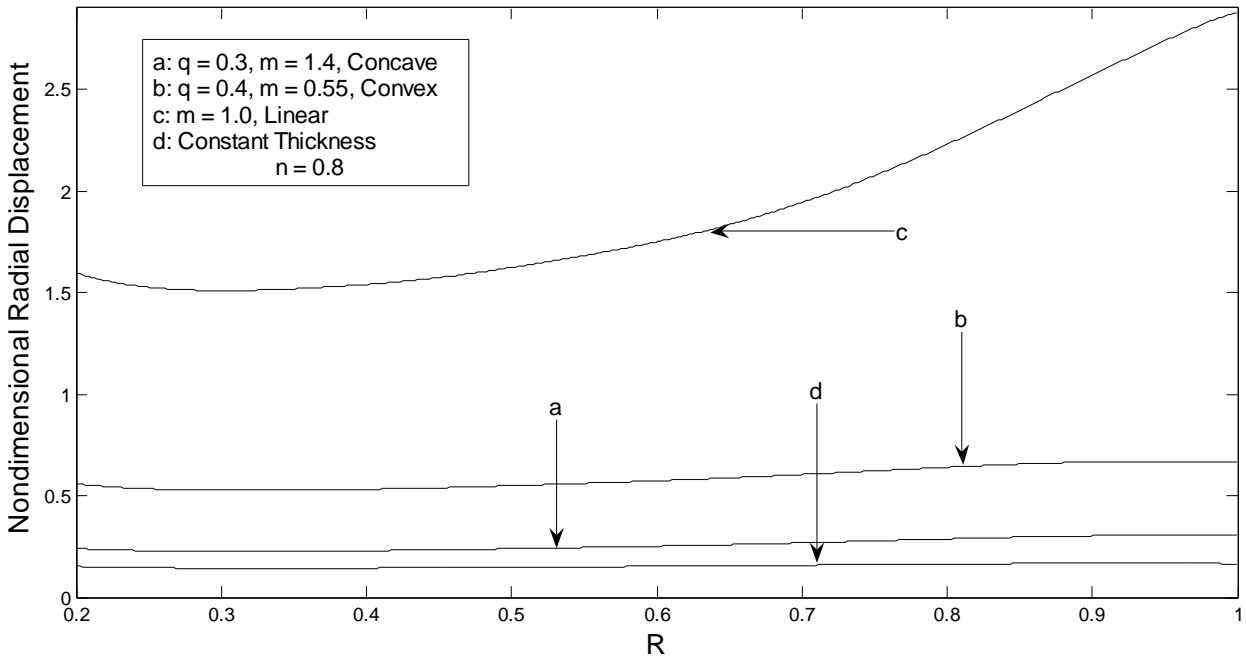


Figure 7. Variation of U versus R for free-free hollow disk in the FG disk with variable thickness for different values of the geometric parameters q and m .

and radial displacement, respectively for different values of the geometric parameters q , m and the grading index n .

In Figure 5, the effect of thickness profile on the radial stress is shown by fixing the value of the grading index, in this case $n=0.8$ and considering different thickness profiles as shown in Figure 2. It is seen that hollow FG disks with uniform-thickness have smaller radial stresses compared to those with variable thickness. FG disk with concave thickness profile is seen to have smaller stress for the chosen values of the geometric parameters q and m in comparison to other variable thickness profiles. Figure 6 shows the effect of grading index n on the stress distributions. It can be seen that the maximum of non-dimensional radial stresses are highest for full-ceramic disk and lowest for full-metal disk and the maximum value of the radial stress for different S-FG disks occur in between. It is noticed that close to the inner surface for the specific values of the grading index n ($n=0.8$), the radial stresses for combination of two S-FG disks may not lie in between the stresses for full-ceramic and full-metal disks but toward the outer surface, the stresses for S-FG disks can be lie in between.

The variation of the radial displacement with radius is shown in Figures 7 and 8. Figure 7 shows the effect of the thickness profile on the radial displacement for the same value of the grading index $n=0.8$ and for different thickness profiles. It is observed that the radial

displacement for the S-FG disk with concave profile thickness is smallest in comparison with other thickness profiles that is, linear or convex. Figure 8 shows the effect of grading index, n , on the radial displacement for all the disks with the same concave thickness profile as shown in Figure 2 but having different grading index. As expected, the radial displacement values for full-metal (Aluminum) disk are greater than those for full-ceramic (Zirconia) disk due to higher modulus of elasticity of the latter. It is noticed that close to the outer surface the radial displacements for S-FG disks lie in between the stresses for full-ceramic and full-metal disks but toward the inner surface, for the specific values of the grading index n ($n=2.0$) the displacements for S-FG disks can be even larger than the radial displacement for full-metal disk. It is worth mentioning that near to full metal surface, inner or outer; the radial displacement varies by, increasing or decreasing, the radius, respectively.

The results of Figures 5 to 8 can be summarized to conclude that, for the same value of grading index, n , the hollow S-FG disk with concave thickness profile is better than those with other variable thickness profiles. This result is similar to the one reported by Eraslan (2003).

Hollow disk (Fixed-free)

The stress distributions for S-FG disk with variable thickness mounted on a rigid shaft for different values of

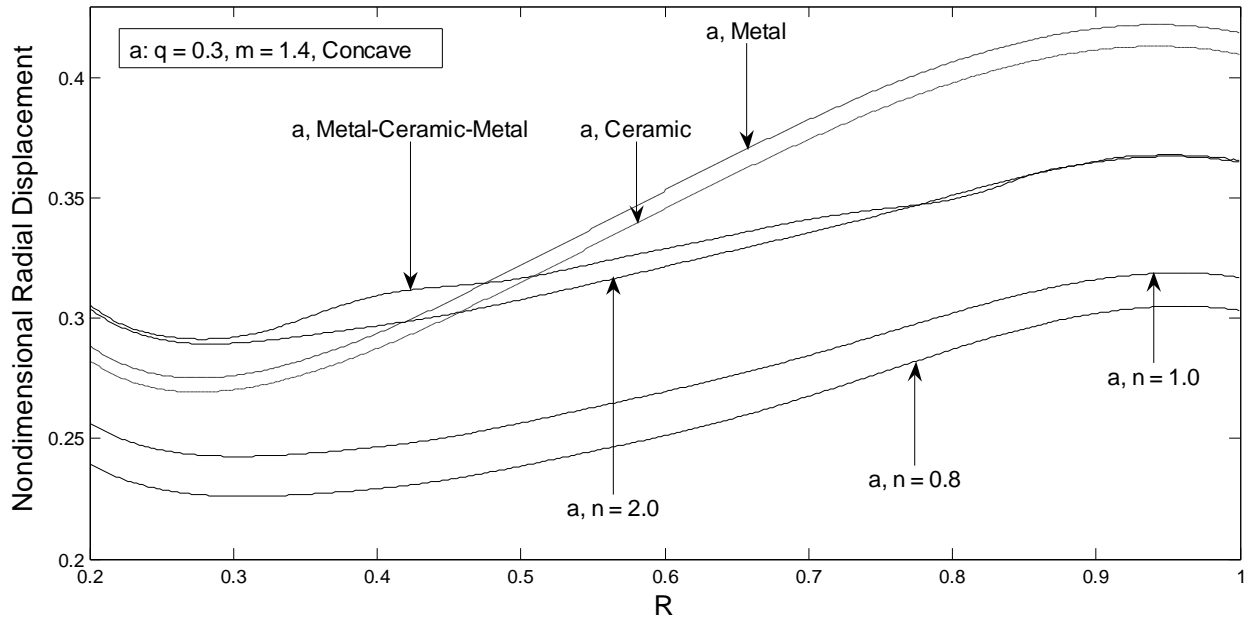


Figure 8. Variation of U versus R for free-free hollow disk in the disk with concave thickness profile for different values of the grading index n .

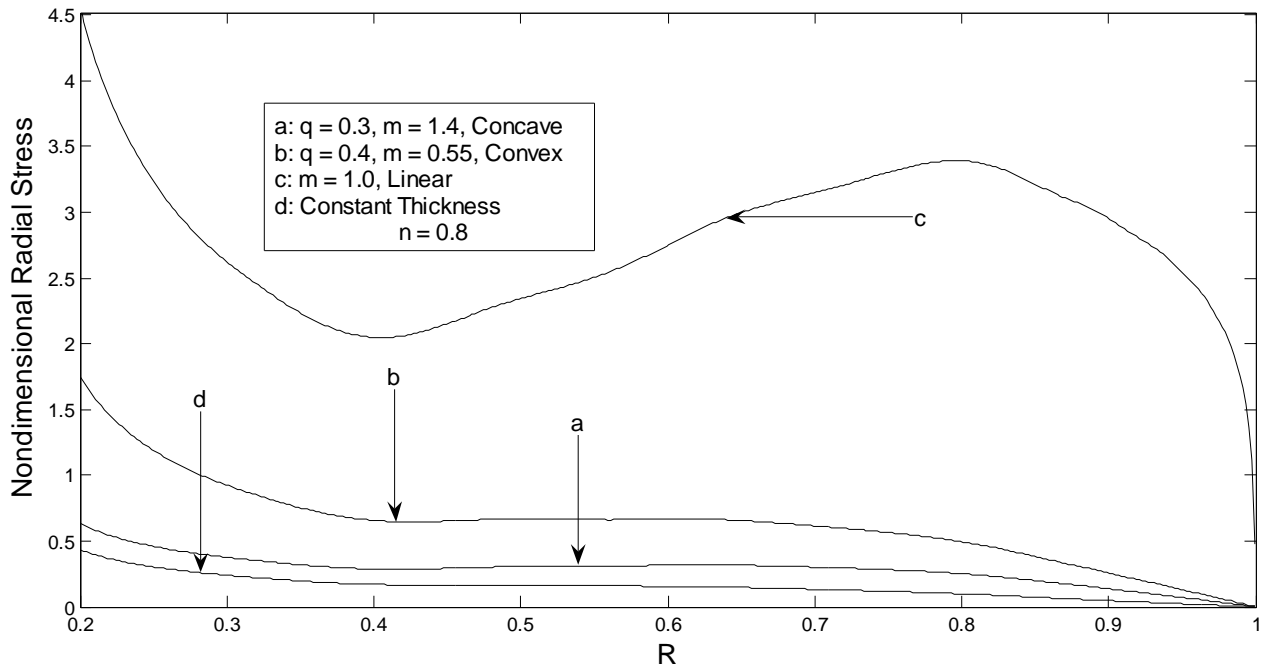


Figure 9. Variation of $\bar{\sigma}_R$ versus R for fixed-free hollow disk in the FG disk with variable thickness for different values of the geometric parameters q and m .

the geometric parameters q , m and the grading index n are shown in Figures 9 and 10.

It is shown in Figure 9 that for the same value of

grading index n ($n=0.8$) the maximum value of the radial stress, for each thickness profile from four cases (a), (b), (c) and (d), occurs at the inner surface

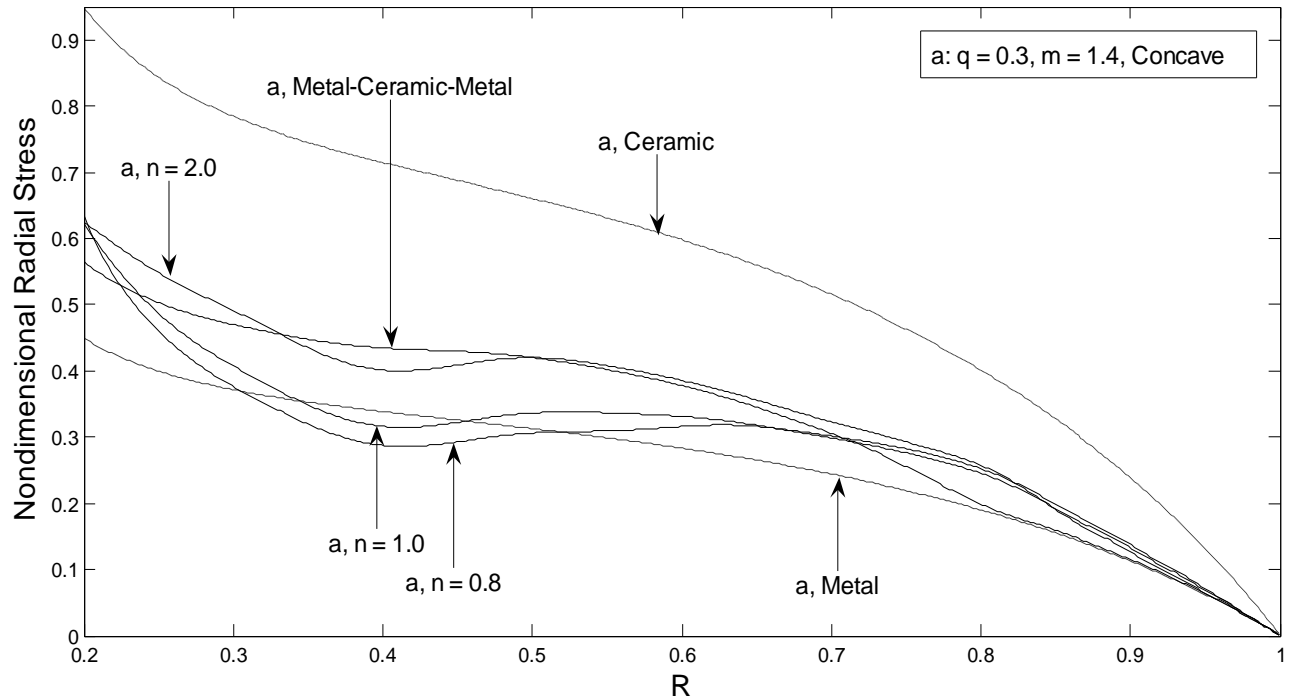


Figure 10. Variation of $\overline{\sigma_r}$ versus R for fixed-free hollow disk in the disk with concave thickness profile for different values of the grading index n .

and each of them is greater than its corresponding value with free-free condition shown in Figure 5. Here again a concave disk is found to have maximum radial stress smaller than other disks with variable thickness. It can also be seen that mounted S-FG disks with uniform-thickness have smaller radial stresses compared to those with variable thickness. Figure 10 shows the effect of grading index n (Figure 4) on the radial stress distributions for S-FG disk with concave thickness profile mounted on a rigid shaft. It is noticed from all the cases considered for different n that for the specific value of the grading index $n=0.8$, the radial stress is smaller than that of full metal disk. Taking into account the boundary condition, this phenomenon can be explained by the presence of interactive effects between stiffness and the centrifugal force due to constant angular velocity of the disk. Figure 2 may be referred to for more details. It is seen near to full-ceramic surface ($r/r_o = 0.6$), the radial stress is constant.

The variation of radial displacements with radius in disks having same grading $n=0.8$ but different thickness profiles (Figure 2) is shown in Figure 11. It is observed that the radial displacement in S-FG disk with concave thickness profile is smaller compared with disks with linear or convex profiles. It is also observed that if the value of n is kept fixed, in the present example, at $n=0.8$ then the FG disks with uniform constant

thickness have smaller radial displacements than the disk with variable thickness. It is shown from Figure 12 that the full-ceramic or full-metal mounted disks have smaller or bigger displacements compared to S-FG disks.

Comparison between metal-ceramic, metal-ceramic-metal and ceramic-metal

For a future investigation, another comparison between non-dimensional displacement for one S-FGM (metal-ceramic or ceramic-metal) and two types of S-FGM (metal-ceramic-metal) are shown in Figure 13.

The variation of the radial displacement with radius is shown in Figure 13. It shows the effect of combination two S-FG disks on the radial displacement for the same value of the grading index $n=1.0$ and for concave thickness profiles. It is observed that the maximum radial displacement for the two S-FG disks with concave profile thickness is smallest in comparison with one S-FG disk (metal-ceramic or ceramic-metal). As expected, the radial displacement values for metal-ceramic disk are greater than those for ceramic-metal and metal-ceramic-metal. It is noticed that close to the inner surface the radial displacements for S-FG disks (ceramic-metal) is smaller than metal-ceramic-metal disk but toward the outer surface the displacements for combination of two S-FG disks can be even smaller than the radial displacement

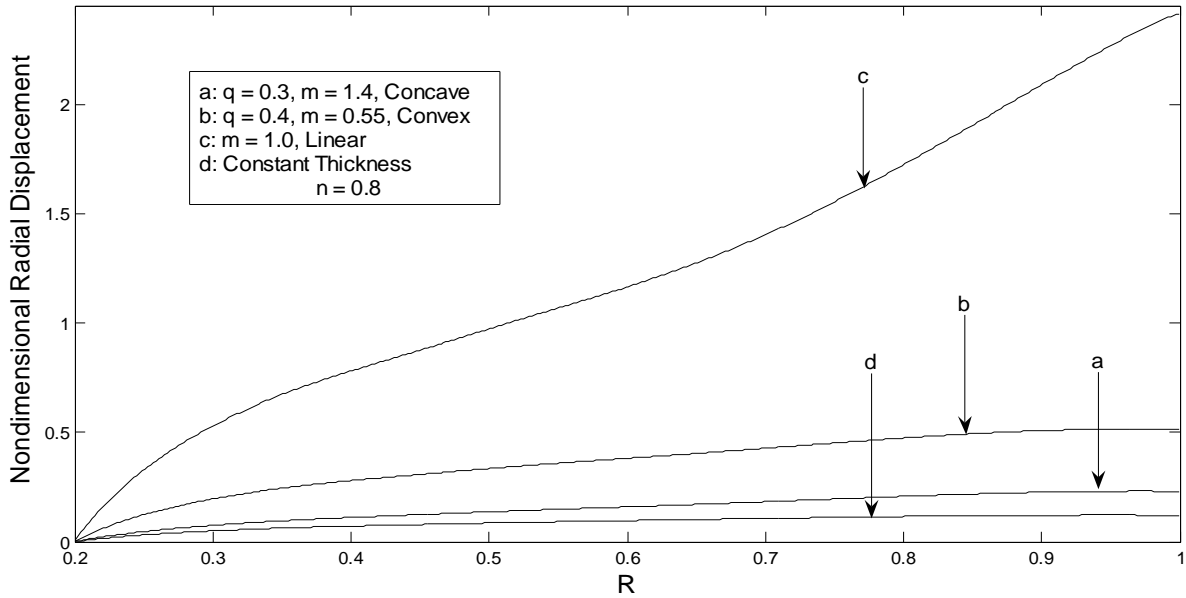


Figure 11. Variation of U versus R for fixed-free hollow disk in the FG disk with variable thickness for different values of the geometric parameters q and m .

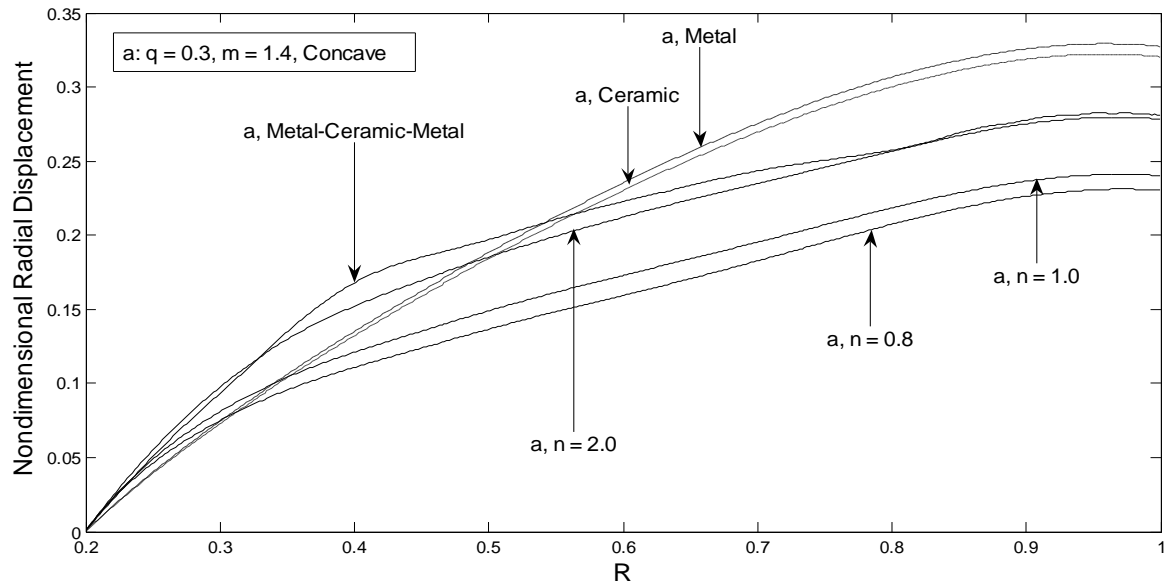


Figure 12. Variation of U versus R for fixed-free hollow disk in the disk with concave thickness profile for different values of the grading index n .

for one S-FG disk.

CONCLUSIONS

An analysis of FG rotating disks with variable thickness is

presented. Combinations of two S-FGMs with hyperbolic thickness profile type are considered. Elastic radial stresses and radial displacements for the hollow disks with both free-free and fixed-free boundary conditions are obtained. The effects of the grading index, n , and geometry of the disk based on different thickness profiles

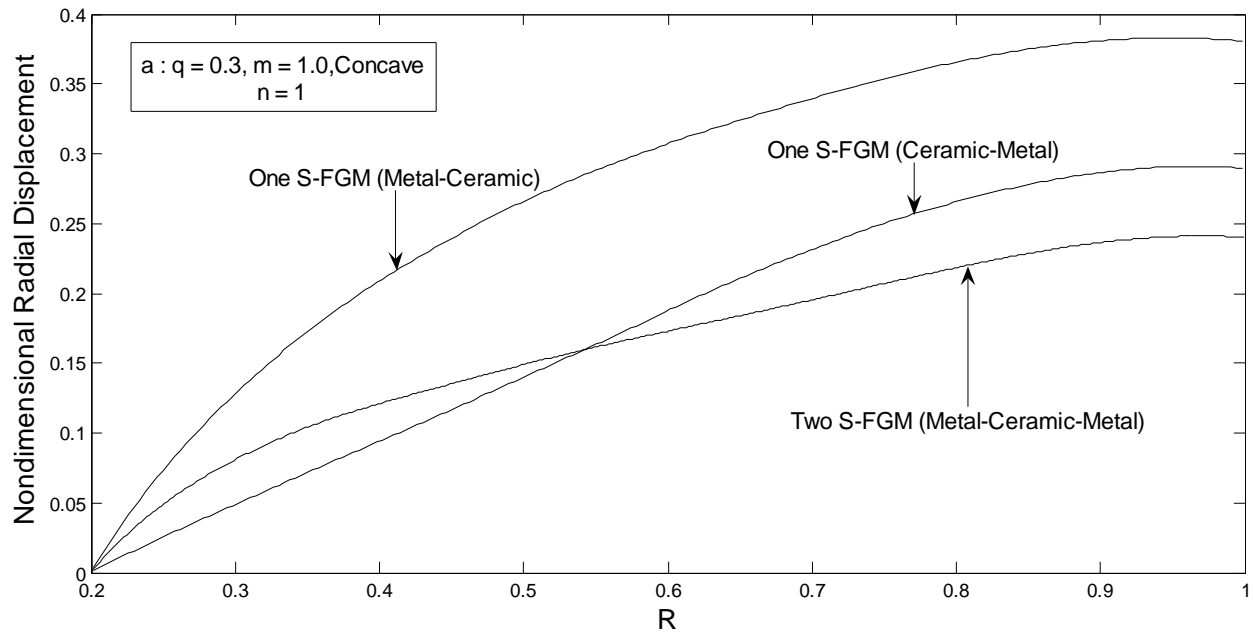


Figure 13. Variation of U versus R for fixed-free hollow disk in the disk with concave thickness profile for different type of S-FGM.

on the stresses and the radial displacements are investigated. Numerical results are presented for the S-FG disk using aluminum as the inner and outer surface-metal and Zirconia at mean radius of disk. These results are compared with those for rotating disks with uniform thickness.

Some salient conclusions of this study can be summarized as follows:

- 1) For the same grading index, n , linear thickness profile is the lightest disk followed by convex, concave and constant, respectively.
- 2) The combination of two S-FG disks with concave thickness profile has smaller stresses than with linear or convex thickness profile while the same grading is considered for all the disks.
- 3) For each of thickness profiles, the radial stress in S-FG disks increases with increase in n by certain radius, after that certain radius the radial stress in S-FG disks decrease with increase in n . Furthermore, for some specific values n ($n=0.8$) the radial stress in S-FG disks are smaller than those in pure material disks.
- 4) For a given pair of materials, there is a particular volume fraction that maximizes a specific mechanical response under centrifugal loading due to constant angular velocity. In other words, free-free or mounted FG disks can have larger radial displacement than full-metal near to the inner surface for some specific grading while maximum values of radial displacements in S-FG disks with variable thickness are smaller than the maximum values for homogenized disks.

5) Hollow rotating FG disks with uniform-thickness profile have smaller stresses and displacements compared to those with parabolic convergent.

6) Maximum radial displacement for fixed-free rotating disk in combination of two S-FG disks is smaller than those in one S-FG disks.

From the semi-analytical results for combination of two S-FG disks given in this study, it can be suggested that an efficient and optimal design of the FG disk calls for a variable section being thicker at the hub and tapering down to a smaller thickness toward the periphery. And also the combination of two S-FG disks can be more effective in comparison with one S-FG disk.

ACKNOWLEDGEMENTS

The authors wish to thank Universiti Putra Malaysia for the financial support to carry out this research and all mechanical and manufacturing department members for their support and helps.

REFERENCES

- Bayat M, Saleem M, Sahari BB, Hamouda AMS, Mahdi E (2008). On the stress analysis of functionally graded gear wheels with variable thickness. *Int. J. Comput. Methods Eng. Sci. Mech.*, 9(2): 121-137.
- Boussaa D (2000). Optimizing a compositionally graded interlayer to reduce thermal stresses in a coated tube. *C. R. Acad. Sci. Paris*, 328: 209-215.
- Chi SH, Chung YL (2006). Mechanical behavior of functionally graded

- material plates under transverse load- Part I: Analysis. *Int. J. Solids Struct.*, 43(13): 3657-3674.
- Durodola JF, Attia O (2000a). Deformation and stresses in FG rotating disks. *Compos. Sci. Technol.*, 60: 987-995.
- Durodola JF, Attia O (2000b). Property gradation for modification of response of rotating MMC discs. *J. Mater. Sci. Technol.*, 16: 919-924.
- Eraslan AN, Argeso H (2002). Limit angular velocities of variable thickness rotating disks. *Int. J. Solids Struct.*, 39: 3109-3130.
- Eraslan AN, Orcan Y (2002). Elastic-plastic deformation of a rotating solid disk of exponentially varying thickness. *Mech. Mater.*, 34: 423-432.
- Eraslan AN (2003). Elastic-plastic deformations of rotating variable thickness annular disks with free, pressurized and radially constrained boundary conditions. *Int. J. Mech. Sci.*, 45(4): 643-667
- Fukui Y, Yamanaka N, Wakashima K (1993). The stresses and strains in a thick-walled tube for functionally graded material under uniform thermal loading. *JSME Int. J. Ser. A*, 36: 156-162.
- Güven U (1992). Elastic-plastic stresses in a rotating annular disk of variable thickness and variable density. *Int. J. Mech. Sci.*, 34: 133-138.
- Horgan CO, Chan AM (1999). The stress response of functionally graded isotropic linearly elastic rotating disks. *J. Elastic.*, 55: 219-230.
- Jabbari M, Sohrabpour S, Eslami MR. (2003). General Solution for Mechanical and Thermal Stresses in a Functionally Graded Hollow Cylinder Due to Nonaxisymmetric Steady-State Loads. *J. Appl. Mech.*, *Trans. ASME*, 70: 111-118.
- Jahed H, Farshi B, Bidabadi J (2005). Minimum weight design of inhomogeneous rotating discs. *Int. J. Press. Vessels Piping*, 82: 35-41.
- Kordkheili SAH, Naghdabadi R (2007). Thermo elastic analysis of a functionally graded rotating disk. *Compos. Struct.*, 79: 508-516.
- Liew KM, Kitipornachi S, Zhang XZ, Lim CW (2003). Analysis of the thermal stress behavior of functionally graded hollow circular cylinders. *Int. J. Solids Struct.*, 40: 2355-2380.
- Ootao Y, Tanigawa Y (1999). Three-dimensional transient thermal stresses of functionally graded rectangular plate due to partial heating. *J. Therm. Stress*, 22: 35-55.
- Ootao Y, Tanigawa Y (2004). Transient thermoelastic problem of functionally graded thick strip due to non-uniform heat supply. *J. Compos. Struct.*, 63: 139-149.
- Orcan Y, Eraslan AN (2002). Elastic-plastic stresses in linearly hardening rotating solid disks of variable thickness. *Mech. Res. Commun.*, 29: 269-281.
- Reddy JN (2000). Analysis of functionally graded plates. *Int. J. Numer. Meth. Eng.*, 47: 663-684.
- Reddy TY, Srinath H (1974). Elastic stresses in a rotating anisotropic annular disk of variable thickness and variable density. *Int. J. Mech. Sci.*, 16: 85-89.
- Reddy JN, Wang CM, Kitipornchai S (1999). Axisymmetric bending of functionally graded circular and annular plates. *Eur. J. Mech. A/Solids*, 18: 185-199.
- Ruhi M, Angoshtari A, Naghdabadi R (2005). Thermoelastic analysis of thick-walled finite-length cylinders of functionally graded materials. *J. Therm. Stress.*, 28: 391-408
- Shahsiah R, Eslami MR (2003). Thermal buckling of functionally graded cylindrical shell. *J. Therm. Stress.*, 26: 277-294
- Suresh S, Mortensen A (1998). *Fundamentals of functionally graded materials. Fundamentals of functionally graded materials.* IOM Communications Limited, London.
- Tutuncu N (1995). Effect of anisotropy on stresses in rotating discs. *Int. J. Mech. Sci.*, 37(8): 873-881.